EXTENDED URBAN TRAFFIC STATE ESTIMATION USING DIFFERENT SENSOR STRATEGIES

Alexander Kutsch, Corresponding Author
Chair of Traffic Engineering and Control, Technical University of Munich (TUM)
Arcisstrasse 21, 80333 Munich, Germany
alexander.kutsch@tum.de
ORCiD: 0000-0002-2001-1140

Allister Loder
Chair of Traffic Engineering and Control, Technical University of Munich (TUM)
Arcisstrasse 21, 80333 Munich, Germany
allister.loder@tum.de
ORCiD: 0000-0003-3102-6564

Gabriel Tilg
Chair of Traffic Engineering and Control, Technical University of Munich (TUM)
Arcisstrasse 21, 80333 Munich, Germany
gabriel.tilg@tum.de
ORCiD: 0000-0001-9167-0680

Klaus Bogenberger
Chair of Traffic Engineering and Control, Technical University of Munich (TUM)
Arcisstrasse 21, 80333 Munich, Germany
klaus.bogenberger@tum.de
ORCiD: 0000-0003-3868-9571

XXX0 Word Count: 6264 words + 3 table(s) $\times$ 250 = 7014 words

Submission Date: August 1, 2022

ABSTRACT

Urban traffic state estimation usually describes flow, density and speed. However, urban traffic is characterized by many factors that cannot be adequately and explicitly described by these parameters alone, yet they are implicitly considered in their values: stopped buses and delivery trucks or an increased number of lane changes affect urban traffic flow. Consequently, the joint estimation of these factors together with the traffic state is valuable for obtaining an extended, more informed traffic state. Applications of such an extended traffic state can be found in traffic management and control or for providing travel information for routing and navigation, e.g., where to expect more stopped vehicles during a specific period of time. The availability of complete trajectory data that continuously represent all motorized traffic participants for a certain period of time allows to better observe these link-microscopic parameters. In this work, we propose a way to estimate the macroscopic values of flow and density as well as the collective number of stops of delivery trucks, taxis and buses, and the number of lane changes are estimated using a physics informed neural network. The network's input are different static and dynamic parameters at the link level to obtain the extended traffic state. Using the data and the network, different sensor distribution scenarios of loop detectors and trajectory data collection are explored to find the optimal sensor distribution for the extended traffic state estimation.

The source code is available at https://github.com/AlexanderKutsch/TRB_Extended_TSE.git

Keywords: traffic state estimation, extended information on urban traffic states, sensor distribution

INTRODUCTION

Traffic in modern cities is highly complex in its nature. The emergence of more and more modes, such as e-scooters, different types of bicycles, etc., is leading to additional interactions in urban space and more competition for road space. Furthermore, the increase in deliveries (online shopping, errands) is leading to increased levels of stops of delivery vehicles on urban streets. All these factors make the estimation and interpretation of traffic states more challenging. The traffic state is commonly referred to as the traffic density (k), traffic flow (q), and speed (v) on a link. As the heterogeneity of urban traffic is only implicitly considered in these traffic states, but not explicitly, decision-making could be wrongly informed. Capturing this information is a rather difficult task, since with the existing sensors it is almost impossible to detect. Approaches to automatically find anomalies, such as accidents, from video data exist, e.g. in (*1, 2*), but they are limited to stationary video data and are not available for use with common sensors. For example, traffic control or routing applications could act differently when the measured speed results from congestion rather than from a higher number of events like lane changes or stops. Thus, only with solid knowledge on the traffic state itself and its enrichment with further factors influencing urban traffic, authorities can design and operate traffic management to increase traffic safety and efficiency while reducing traffic emissions. In addition, routing platforms can provide better services.

The main data for traffic state estimation (TSE) are loop detectors (LD) and floating car data (FCD) (*3*). As these data are usually not available continuously everywhere, the data availability and combination of different sources are not only determining the estimation method, but also the estimation quality (*4, 5*). The canonical methods for TSE were first developed for freeways. Existing approaches using filters, such as the Extended Kalman Filter (*6*) and an extension using a first-order model of traffic flow (*7*) or using a spatio-temporal lowpass filter (*8*) were developed with data from LD only. A further approach with FCD and a Kalman Filter was proposed by (*9*). Also combinations of LD and FCD using an extended Kalman Filter (*10*), as well as data-driven methods were developed (*11*). Since machine learning has become more and more popular due to higher data availability, these methods have also been used for some time, e.g. (*12*). A comprehensive literature review on freeway TSE is provided by Seo et al. (*3*). For the more complex case of urban TSE, methods exist as well, also based on available data from LD, FCD and GPS data from buses and taxis and different scenarios for combining them. The concepts make use of various models, which are partially also used for freeway TSE, such as the LWR-model (*13*), multiple regression (*14*) or speed transition matrices (*15*). Also new data sources, e.g., connected vehicle communication were used for signalized links (*16*). Besides that, also machine learning and in particular deep learning models were used, a review can be found in (*17*).

Describing complicated matters and non-linear relationships in urban traffic situations makes the application of traffic control measures difficult. For this purpose, traffic is often simulated and predicted by means of simulators, which, however, are complex to calibrate, require high computing power and are often expensive. One potential solution are data-based approaches utilizing machine learning methods. These are increasingly being acknowledged in the field of transportation (*9*). Lately, deep learning methods have advanced towards the modeling of physical systems (*18–21*). These advances utilize the information contained in the differential equations of the physical system to regularize or constrain the learning process, e.g., the continuity equation for fluids. This approach could be valuable for traffic state estimation, since many traffic flow models include differential equations (e.g. LWR), which has already been shown recently (*22–25*). They were compared to canonical TSE methods and their superiority was shown (*26, 27*). The application of

physics-informed but data-based TSE was also shown to be beneficial for the use case of fusing LDD and FCD (*28*). Furthermore, a simple approach was proposed that combines the fundamental diagram and a widely used data-driven technique to develop an explainable physics-informed and data-driven TSE approach based on loss constraints (*29*).

What to the best of our knowledge is still missing are models that capture not only the speed, density and flow on urban streets, but also the more complex events causing flow reductions and time losses. Measurements of such events do already exist, but are limited to local anomaly detection and not used in the context of TSE. Furthermore, there is no possibility to determine such events on the basis of permanently and ubiquitous available sensor data like LD and FCD.

In this paper, we propose the concept of an extended traffic state (EST) and show its estimation in practice. Using the seminal pNEUMA data (*30*), we describe the proposed extended traffic state and show its estimation using a physics-informed deep learning approach. We examine the estimation results under five different sensor scenarios, including LD, FCD and trajectory data from buses and taxis. The proposed procedure of learning the estimation parameters from drone trajectory data is already a step forward to standardization and reproducibility; the employed estimation and data collection methods are increasingly becoming widely recognized and available to many, supporting to scale and reproduce the extended traffic state estimation at various locations.

EXTENDED TRAFFIC STATE WITH LANE CHANGES AND STOPPING BEHAVIOR

For dense urban areas, traffic is a strongly heterogeneous entity (*31*). Slow modes of transport interact with faster vehicles, disturbing influences due to traffic lights, parking vehicles, delivery stops, bus stops and many more occur permanently and have impact on traffic flow and infrastructure for leisure and vulnerable road users make the situation more complex (*32, 33*). Canonical TSE methods aim for estimating either the flow, density or speed in a network using different attempts with either flow models, data-based methods or a combination of them. However, the three variables cannot fully represent the complexity of urban traffic. Phenomena that exist but have not yet been measurable on a macroscopic scale thus remain unaddressed. With complete trajectory data sets, however, it is now possible to extract this information and use it in control and planning applications. An extension of the canonical parameters can be made to include the collective number of stops of delivery trucks, as well as taxis and buses for passenger boarding or alighting. A possible application is to include this information in the routing process. In addition, the number of lane changes in a road section is another possible aspect that provides information that is relevant to traffic safety and can be used for planning. The difference between the canonical traffic state estimation and the extended traffic state estimation is highlighted in Figure 1. The aspects mentioned above are core subjects in traffic engineering. For lane changes, for example, the detection and prediction for the driving task in autonomous driving (*34*), as well as the development of simulation models (*35, 36*) are prime analysis examples. The effects of bus stops on urban capacity has also been investigated, e.g., (*37*), as well as the automated detection of incidents on roads. e.g., (*38, 39*). However, these parameters have not yet been used as additional information as an output of TSE.

Data for the extended traffic state estimation

To illustrate the extended traffic state estimation, we use the seminal pNEUMA data (*30*). In the frame of this experiment, vehicle trajectories were extracted from videos recorded during the morning hours of five weekdays by a swarm of ten drones. As Figure 2A shows, the number of

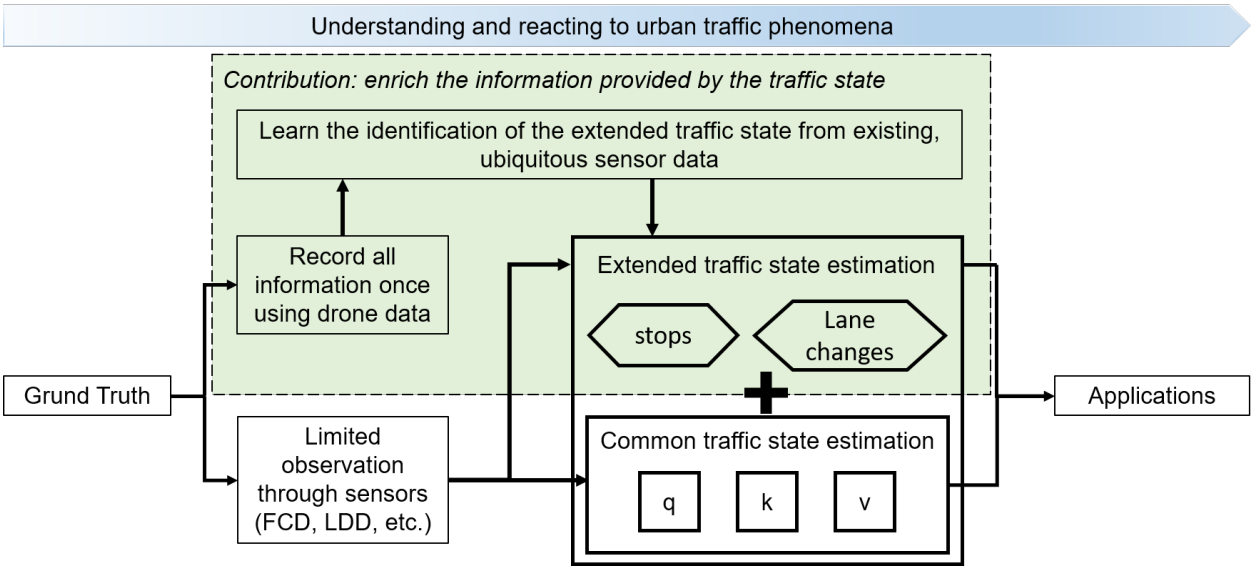

FIGURE 1: Extending existing approaches for traffic state estimation in urban areas by extending it with further information on stops of delivery vehicles, taxis and buses and lane changes.

different vehicle types in the pNEUMA experiment is high. Cars have the highest share of around 42%, but also the combined share of likely slower vehicles, specifically medium vehicles, heavy vehicles and buses is at about 7.5%. These modes have, as visible in Figure 2B, the lowest mean speeds per vehicle, as well as the lowest quantile values. Analogously, the outliers also do not reach the values of Cars, Motorcycles and Taxis. Therefore, the complexity embedded in this data and the fact that it provides ground truth information makes this data perfectly suitable to show the extended traffic state estimation. In addition, as such drone data is becoming more and more widely available and the data processing standardized, the methods can easily be used and transferred to further data.

Besides that, a closer look into the stopping behavior shows that stopping of vehicles might have various reasons. As shown in (*33*), during the experiment in Athens, buses and freight vehicles have a higher stopping frequency than private cars, with buses having the highest frequency. In general, freight vehicles cannot be distinguished directly from the data set, but are likely to be medium and heavy vehicles, as discussed by the authors. Besides that, of course the stopping of buses, just like taxis that let passengers get on and off at the edge of the roadway may have an impact on traffic flow variables. Further implications might come from a slower acceleration at the stop line of a traffic light after a red signal. From Figure 3 the places of stopped vehicles on a exemplary link show that most of the stops are based on the right most lane, likely due to drop on- and off events, as well as in front of the stop line. The parameters for a vehicle to be considered as stopped in this case were chosen in a way that a vehicle drives less then $1 km/h$ for a minimum duration of at least $5 seconds$, while the mean speed of the cars on the link was equal to or higher than $20 km/h$. This ensured to exclude the large amount of stops caused by traffic signals or other waiting processes that are not limited to these type of vehicles. On the other hand, the stops of the larger vehicle groups near the stop lines are also included. Especially heavy vehicles and buses, but also medium vehicles tend to have lower acceleration than cars or motorcycles. Consequently, they force upstream vehicles to temporarily reduce their speed up to standstill, or

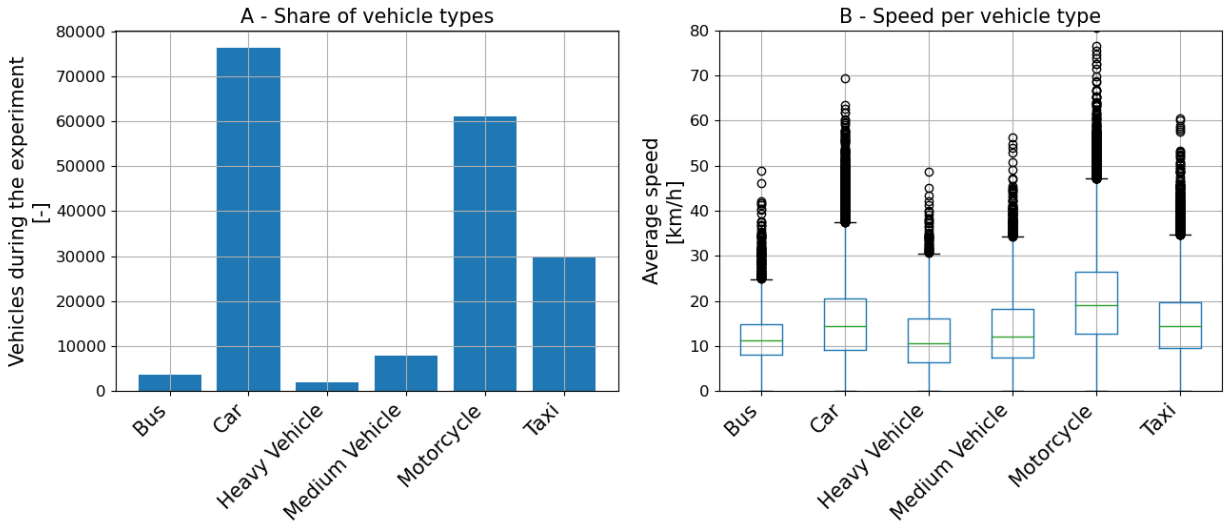

FIGURE 2: The share of vehicles in the pNEUMA experiment (A) and boxplots of the mean speeds per vehicle type (B).

prevent them from accelerating as fast as intended, depending of whether they arrive at the end of a queue during a green phase or they are currently stopped at a red light. In this way, they act as moving bottlenecks, i.e. they continue to move in space, but generate velocity losses upstream, which are recovered when the moving bottleneck is passed (*40*).

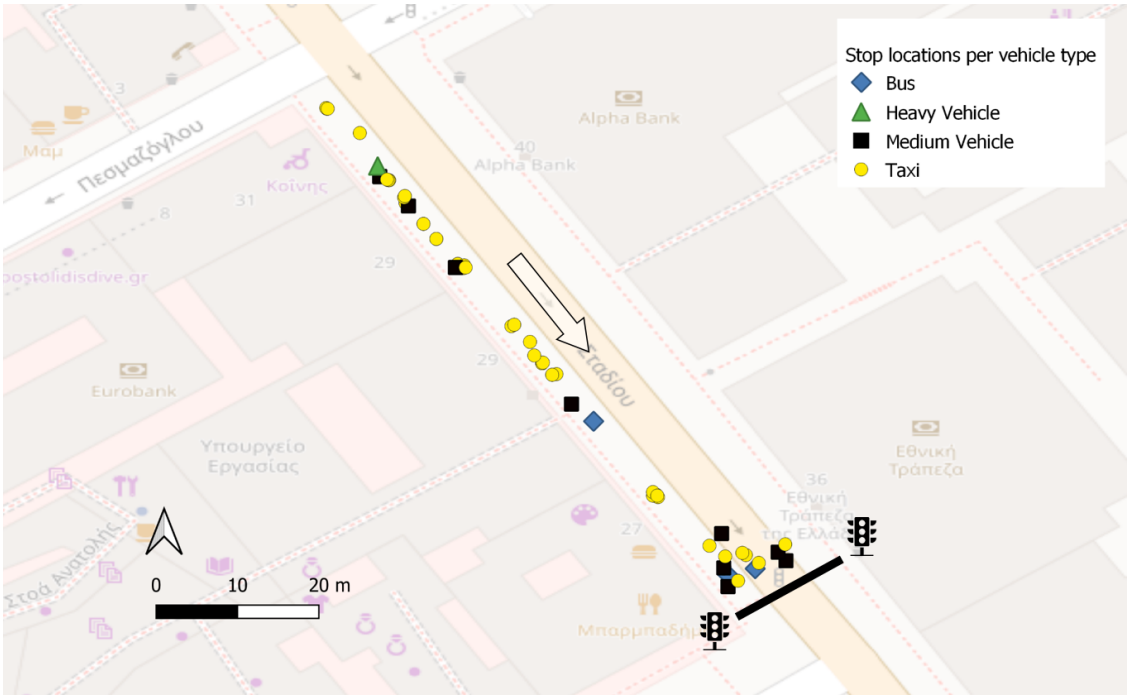

FIGURE 3: Place of stops of medium and heavy vehicles, taxis and buses, exemplary for a link on the 'Stadiou' street.

A second substantial impact on traffic flow and safety are lane changing maneuvers. Although, probably due to a lack of available data, this effect has mainly been investigated on freeways, e.g. (*41*), the availability of big data sets in urban areas led to a gained interest here as well (*42*). Consequently, dense, inner-urban traffic contains far more information than is used for current methods of TSE and, accordingly, traffic control. To aggregate this complex composition into further measurable, sort of meta variables, we propose to include the amount of lane changes and the number of stops of the shown vehicle types in Figure 3, in the following called special vehicles.

PROCEDURE FOR ESTIMATING EXTENDED TRAFFIC STATES

The entire process of extended TSE starts with the recording of videos of the traffic, most likely with drones. From this, the trajectories of the required road users are extracted and classified, in the example of pNEUMA these are all motorized vehicles. From this data set the ground truth can then be determined, for the canonical TSE these are the flow, density and speed. In our approach, these are extended by the number of lane changes and the number of stops of special vehicles. Depending on the available real detectors, the corresponding data can be generated virtually. For example, a virtual LD can be generated to simulate the data that a real LD would generate. Any suitable functional form for a regression approach can then be chosen to determine the extended TSE. The method can be calibrated and validated by comparing the results with the ground truth data. The process is summarized in Figure 4. The proposed method is spatially based on link-level and up to date limited to the estimation of the extended traffic state, meaning no prediction is possible to that point. Consequently, calibration is performed using individual streets in a network within the area covered by the aerial survey.

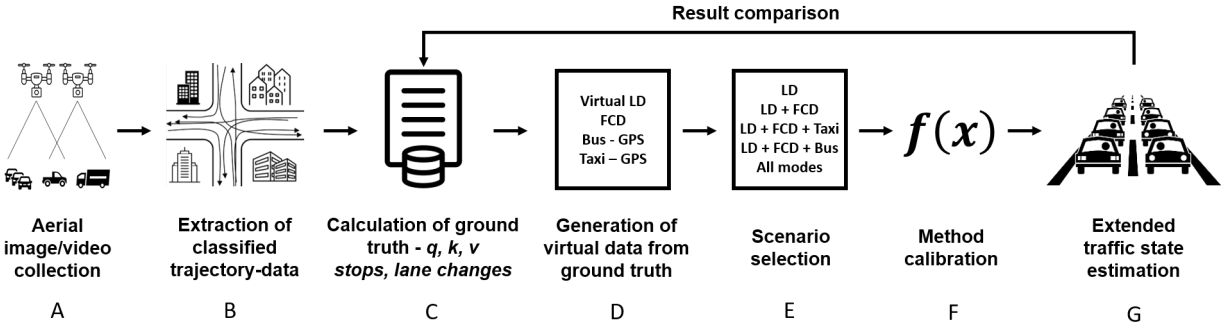

FIGURE 4: Process overview over the extended TSE with ground truth data.

The method is directly applicable once a function is calibrated with the acutal sensor distribution available. Thus, from the abundant data, the extended traffic state can be estimated using only permanently available sensors and data, such as LD and FCD. With this additional information, for example, routing can be improved and made more individual. For example, it is conceivable to increase the cost function of links by the number of stops of special vehicles. The same applies to the number of lane changes, which, in addition to the possible effect on traffic flow and bottlenecks, can also be critical to safety. The information can therefore also be helpful for planning aspects. A prerequisite for the application is that a complete ground truth data is available for calibration. Also, because of the link level basis, the method is efficiently scalable.

DATA PROCESSING AND EVENT LABELLING

The data available on the experiment's web page was processed in the following way to serve as an input for this study. The original files were reshaped to a long data format and the step width was enlarged from 0.04 seconds to 0.16 seconds, to keep the relevant information, but thin the data set somewhat for faster compatibility. Furthermore, the data was joined into a single file, making unique ids per vehicle by combining the experiment number and the track id, as well as the travelled distances were calculated and a global timestamp added. Afterwards eleven links were selected, shown in Figure 5, based on a spatial filtering of the coordinates. For each experiment, the first and last 60 seconds were removed from the data, while experiments 8 was completely removed due to observed anomalies. Moreover, parked vehicles, i.e., having a travel distance within a link that covers less than 10% of the link length during the whole flight period, non-motorized road users, as well as vehicles moving in the wrong directions were removed from the data.In a last processing step, in order to elicit effects induced by the different phases of the traffic signals, the information was temporally aggregated. At the time of the recordings in Athens, the cycle time of the traffic signals was mostly about 90 seconds. Using a time span of two cycle lengths, i.e. three minutes was chosen, which is updated every 30 seconds.

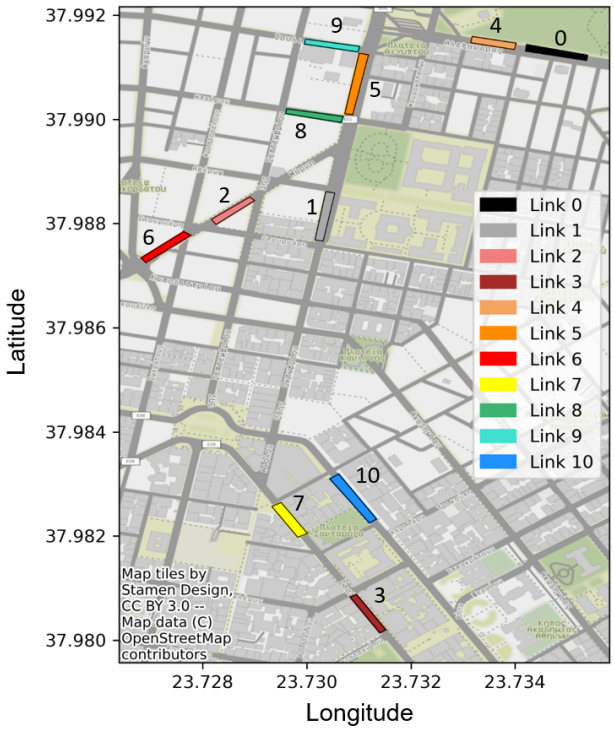

FIGURE 5: Selected links in the city center of Athens, covered by the pNEUMA experiment.

The input into the method consists of static and dynamic variables. The static input parameters describe the street layout and were extracted using Google Maps and Open Street Maps. The dynamic input parameters describe the traffic itself and change over time. The FCD, as well as the ground truth flow and density per vehicle type were calculated using Edie's definition (*43*) for each 30 second interval, which are afterwards aggregated to 3 minutes, using a rolling average. The calculation of traffic flow there is given by the sum of the travelled distance of each vehicle,

divided by the interval length multiplied by the link length, and the density is given by the sum of the travel times of the vehicles, divided by the same numerator. Lastly the speed can be obtained by dividing the flow by the density. Besides the virtual FCD, also virtual single LD were created, placed 30 meters before the stop line of each street segment. Analogously, flows and occupancies were calculated for the loops, and with this again the densities were calculated under the assumption of an average vehicle length. The difference for the LD is that it was not calculated per vehicle type, but for all modes combined, since single loop detectors cannot distinguish vehicle types. The values from the virtual FCD and LDD are transformed using a linear transformation such that the data of all links can be used in the same extended traffic state estimation model. So all flow and density values were divided by their respective link mean values. Subsequently, the flows were divided by the free-flow velocity. The linear transformation can always be reversed so that the actual link values are obtained.

The determination of stops of the special vehicle types, namely taxi, bus, medium and heavy vehicle, was conducted by assessing the speed parameters for every timestamp on a link, in our case every 0.16 second, on the single trajectory basis. For our method, three parameters are used to identify a stop: (i) the speed of a single special vehicle drops below $1km/h$, (ii) the mean speed of all cars on the respective link, calculated per time step, is beyond a minimum of $15km/h$ and (iii) these conditions last for at least 5 seconds. This prevents most of the stops that appear due to red lights from being classified as such stop, when the vehicles on the link are also waiting in a queue. With this method, still some stops near the stop line are categorized as such, but they appear mainly in the beginning of red phase, implying that they are at the front of the queue, which is why they impede other vehicles that may be accelerating faster. On the other hand, delivery stops and passengers boarding and alighting from buses and taxis are correctly classified as a result. A disadvantage of the condition that the average speed of the cars on the link must be at least $15km/h$ is that delivery stops that last for several cycle times are not recognized as one delivery stop, since the condition is no longer fulfilled during the red phases. However, the temporal aggregation, as well as the fact that only the number of stops but not the stop duration is predicted, takes this fact into account and thus compensates for overlong stop duration by increasing the number of stops.

Although lane assignment methods for the pNEUMA experiment exist (*42*), a simple approach was used for this classification to aim for a easy to scale solution that is extractable from any type of trajectory data set. In a first step, motorcycles were excluded from the consideration of the lane changing behavior. Having a closer look at the data, motorcyclists, especially during red phases, tend to overtake the waiting queue between the designated lanes and the waiting vehicles, and therefore do not really change the lane, nor keep the intended lanes as well. So the focus in this work was on the other vehicle types. In a first step, for every time step, each vehicle was matched to a lane according to its geographical coordinates. A lane change is then simply detected, if the assigned lane number changes. This for some cases still leads to a high number of lane changes for a single vehicle, since there are still some vehicles left, that drive in between the designated lanes, similar to motorcycles, but as Figure 6A exemplary for link 5 shows, these vehicles only make a small share of vehicles. As expected, most of the vehicles do not perform a lane change, and the distribution appears to be exponentially shaped. The lane changing of a vehicle once is quite reasonable, while higher amounts are really rare to expect, especially more than two lane changes. Therefore, for each vehicle the first lane change during an interval on the respective link is counted as such, each additional lane change is considered a measurement error.The resulting proportion of vehicles changing lanes, shown in Figure 6B, varies from link to link, which again supports the

motivation to extract this information.

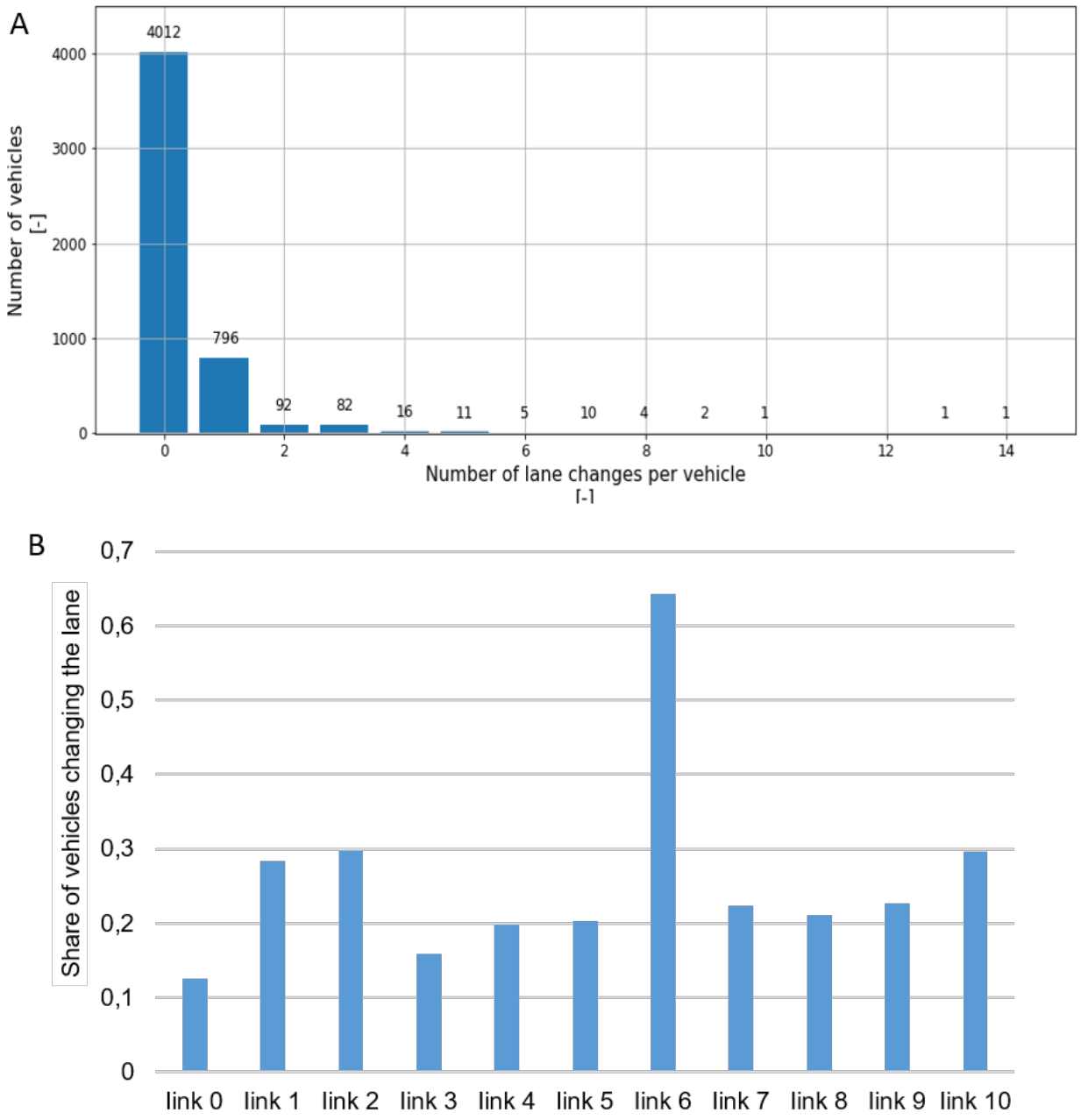

FIGURE 6: The number of lane changes per vehicle on link 5 (A) and the share of vehicles performing a lane change per link (B). Motorcycles are not included due to their low lane discipline, especially in waiting queues.

The number of stops, as well as the number of lane changes are then added to the respective macroscopic observation intervals of traffic flow and density. As can be seen in Figure 1, adding this additional information into the process for estimating the extended traffic state is the first step towards the novelties presented in this paper. Regarding the whole process, the steps are completed up to the generation of virtual data from the ground truth, shown in Figure 4D.

SENSOR DISTRIBUTION AND TRAFFIC STATE ESTIMATION PROCESS

Dynamic Input for extended traffic state estimation

Many different sensors are used to detect road traffic, either stationary permanent or mobile available. Consequently, the obvious question is how to estimate the extended traffic state as accurately as possible with the data available therefrom. To describe realistic sensor distribution or to give at least an insight into an optimal solution for such usage, different combinations of sensors were chosen. For each link, the minimum requirement is that a loop detector is present for the investigated scenarios. This is a single loop, being able to only capture flow and density, but not to distinguish between the different vehicle modes. Moreover, a growing proportion of vehicles are equipped with GPS devices. Thus, a certain amount of FCD, in this case the position and the speed, is available for vehicle manufacturers, navigation service providers or smartphone manufacturers. Therefore, the share of available FCD from cars was assumed to be at 5%. On the reverse, of course, the proportion of equipped vehicles must be known for real-world applications, but can be easily checked by the presence of loop detectors. Besides private cars, also buses and taxis are often equipped to deliver such data. Using these assumptions, the different distributions shown in Table 1 were used for the dynamic input for the extended traffic state estimation.

Scenario 1	Scenario 2	Scenario 3	Scenario 4	Scenario 5
Loop Detector	Loop Detector	Loop Detector	Loop Detector	Loop Detector
-	5% Car	5% Car	5% Car	5% Car
-	-	Taxi	Bus	Taxi
-	-	-	-	Bus

TABLE 1: Different sensor scenarios for extended traffic state estimation.

Static Input variables

The dynamic values give information about the traffic parameters for the considered links, but are hardly usable if additional information about the road layout is not available. The static variables are therefore considered as well. They are link-specific and do not change over time. The considered parameters include information on the link length, the number of lanes, the presence of and the number of bus stops on a link, the presence of a separate lane for buses and the road rank according to Open Street Map, assigning rank 0 for main streets and rank 1 for minor streets. The values of these parameters for the links investigated for our model are listed in Table 2.

Extended traffic state estimation approach

To capture the complex effects in urban traffic, that up to now are not considered for TSE, a neural network approach is chosen. The major advantage of neural networks, that non-linearities are implicitly mapped in the network during the training, leads to a data-driven modelling approach as motivated earlier (*44*). Thus, the use of deep learning should not be understood as a new approach to TSE itself, but as an application tool to solve the problem in the most efficient way. In this paper, we built on recent advances in physics-informed deep learning proposed by Dahmen et al. (*29*). The authors propose a NN, where the input vector consists of the static parameters described in 2, combined with the dynamic input according to the scenario from 1. The output consists of the estimated flow and density, from which the velocity can be calculated via the fundamental

link	length [km]	lanes	bus stops	separate lane	road rank
0	0.105	3	0	1	0
1	0.105	3	2	0	0
2	0.084	2	0	0	0
3	0.09	3	0	1	0
4	0.075	3	0	1	0
5	0.1305	3	0	1	0
6	0.095	2	0	0	0
7	0.079	3	1	0	0
8	0.093	2	1	0	1
9	0.092	2	1	0	1
10	0.121	4	1	0	0

TABLE 2: Static parameters of the eleven inspected links used as input for the TSE.

equation $q = k * v$. The network is physics-informed in a way that the loss used for training has an extra constraint based on the fundamental diagram (FD). More precisely, an estimated FD is used to add an extra penalty to value pairs of q and k that lie above the curve. This aims at filtering for unrealistic data points, especially extremely high speed values, since disturbances in traffic flow may lead to points that are beneath the FD, but are very unlikely to make points shift far above the curve. Therefore, the initial loss function $\mathscr{L}_{MSE}$ (mean squared error) is partially replaced by the physical loss function $\mathscr{L}_{PHY}$, which is composed of $\mathscr{L}^q_{PHY}$ for the flow and $\mathscr{L}^k_{PHY}$ for the density. The parts with the physical loss are calculated as follows:

$$\mathscr{L}^q_{PHY} = \left(Q\left(\hat{k}\right) - \hat{q}\right)^2 \tag{1}$$

$$\mathscr{L}^k_{PHY} = \left(K\left(\hat{q}\right) - \hat{k}\right)^2 \tag{2}$$

with $\hat{k}$ being the estimated traffic density and the $Q(\hat{k})$ the respective point on the fundamental diagram, and $\hat{q}$ being the estimated flow and $K(\hat{q})$ the respective point on the FD for. The loss of the neural network is then calculated with equation 3, where γ describes the extend to which the initial loss function is replaced by the physical loss and n being the amount of batches. As proposed by the authors, γ was set to a value of 0.6, because results seem the most promising regarding speed estimations for this split the between physical and initial loss.

$$\mathscr{L}_{NN} = \frac{1}{2n}\left(\sum_{i=1}^{n}\left((1-\gamma) * \mathscr{L}^q_{MSE,i} + \gamma * \mathscr{L}^q_{PHY,i}\right) + \sum_{i=1}^{n}\left((1-\gamma) * \mathscr{L}^k_{MSE,i} + \gamma * \mathscr{L}^k_{PHY,i}\right)\right) \tag{3}$$

This approach was further developed for our purpose and enhanced by the two parameters. As illustrated in Figure 7, the input factors consist of the static link-specific parameters, together with the dynamic traffic values, depending on the sensor scenario. The output is then the flow and the density on the link, from which speed can then be obtained, as well as the discussed extensions, namely the number of stops and the number of lane changes. Since the physical information using the FD is only valid for the flow and the density, the loss function had to be adjusted accordingly.

Consequently, the two additional output variables were added to the loss using the mean squared error, while the loss from the flow and density is still calculated via euqation 3. Nevertheless, the physics-informed neural network is enlarged with further information from actual traffic. The parameters for the network were left as proposed in the original approach, because a sensitivity analysis for this layout did not yield a significant improvement. The network structure is illustrated in Figure 7, the respective parameters for initialization, training and the layout are listed in Table 3.

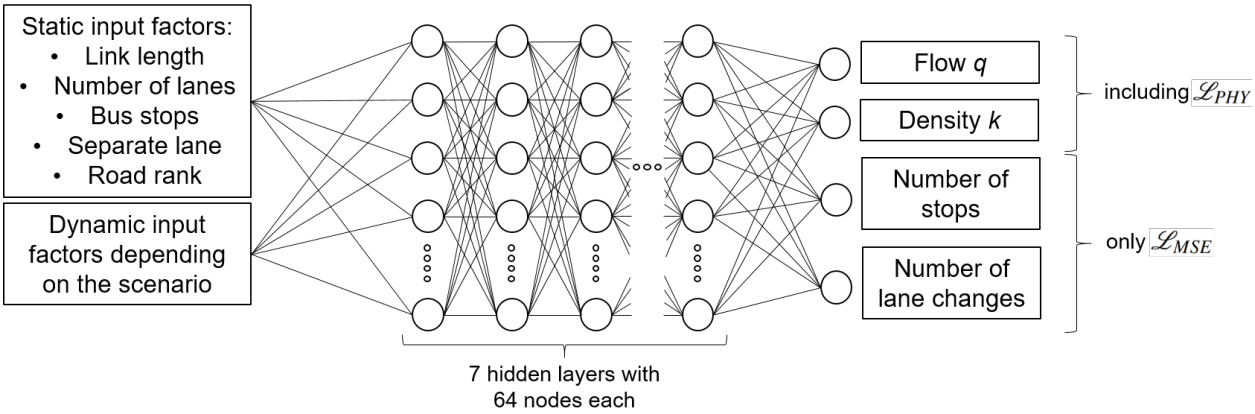

FIGURE 7: Neural network architecture for estimating the flow, density, number of stops and number of lane changes.

Parameter	**Value**
Hidden layers	7
Nodes per layer	64
Learning rate	0.001
Optimizer	Adam
Activation function	LeakyReLu (0.01)
Weight initialization	Kaiming
Batch size	256
Regularization	early stopping, no dropout
training, validation, testing split	0.7, 0.15, 0.15

TABLE 3: Neural network parameters for extended traffic state estimation

RESULTS AND DISCUSSION

The network was trained for each scenario individually and the mean of 20 runs for each was calculated for the results. Since the problem at hand is a regression problem, for the estimation of the flow, the density and the velocity on the one hand the R2 value and on the other hand also the mean average percentage error (MAPE) was determined. For the estimation of the number of stops and the number of lane changes only the R2 value could be measured, because results with a true of zero were included, which makes the MAPE rise to infinite. The R2 score describes the coefficient of determination and is best at 1.0, while a R2-score of 0 would mean that the model estimates

constantly the mean value of the target vector. The MAPE is described by the mean average error between each estimation and the respective actual value in relation to the actual value.

Besides estimating the input flow and density, the calculated speed is compared to the original speed, which is the calculated speed from the input measurements, and the target speed, which is the speed calculated from the flow and density of the input vectors during the respective intervals. They differ slightly due to the resampling of the data from 30 seconds to the three minute intervals.

Estimating Flow, Density and Speed

The R2 values for the flow and the density achieved with the method are in the range of about 0.8 for all scenarios, as can be seen in Figure 8A, and are thus very satisfactory. The best results are obtained for Scenario 3, which includes the LD, 5% of the FCD and the taxi data as input variables, and Scenario 5, including also the bus data. Here, the largest R2 score for flow is about 0.82, and for density about 0.85. Larger differences between the R2 scores are seen when comparing the velocities in Figure 8B. As expected, the target speed is in general estimated slightly better than the original speed, independent of the scenario. Using only the LD as input values results in the worst R2-score of only 0.56. By adding the FCD, a significant improvement can be achieved, resulting in a score around 0.8. By further having the taxi data available, also the score for the velocities is best for Scenario 3, since more available data sources result in better performance. If the taxi data are replaced by buses, as in Scenario 4, the goodness of the estimate drops markedly to R2 values below 0.6. This difference could be caused by the fact that buses usually have a different operational management strategy. There are centrally controlled schedules and target departure times, which is why the behavior differs strongly from the other road users. However, as Figure 2A shows, buses represent only a very small share of vehicles. If buses are equally weighted with the small number of FCDs as input variables, an oversampling of buses is achieved. The outputs are therefore no longer representative of the data set and thus give a worse overall result than if the taxi data are used additionally to the FCD, which represent a significantly larger sample. For scenario 5, where both the taxi and the bus data, together with the FCD and the LD are included, the score is again significantly better, but due to the abnormal behavior of the buses still slightly worse than the scenario without buses.

The values for the MAPE of the estimations support the findings. Scenario 3 has the lowest MAPE for all of the flow, density and velocity estimations, followed by Scenario 5. This again is the expected result, since more available data sources help estimating a better result. Only Scenario 4, including only the buses without the taxis is again having worse results, presumably due to the aspect already discussed.

Estimating the extended parameters: Stops and lane changes

As can be seen from Figure 10, the estimation of the additional parameters, namely the stops of the special vehicles, including the delivery vehicles, taxis and buses, and the lane changes, is worse than the estimation of the canonical parameters. This is probably due to the fact that these situations are rather difficult to measure with the existing sensors, as explained before. Nevertheless, with LD alone, a R2 value in the range of about 0.57 to 0.58 can be obtained for the two parameters. While the score for the number of lane changes does not improve significantly and reaches a maximum of 0.59 for scenario 5, improvements in the estimation of stops are possible. Only a small increase in the score is seen due to the availability of FCD. The addition of taxi data greatly improves the result

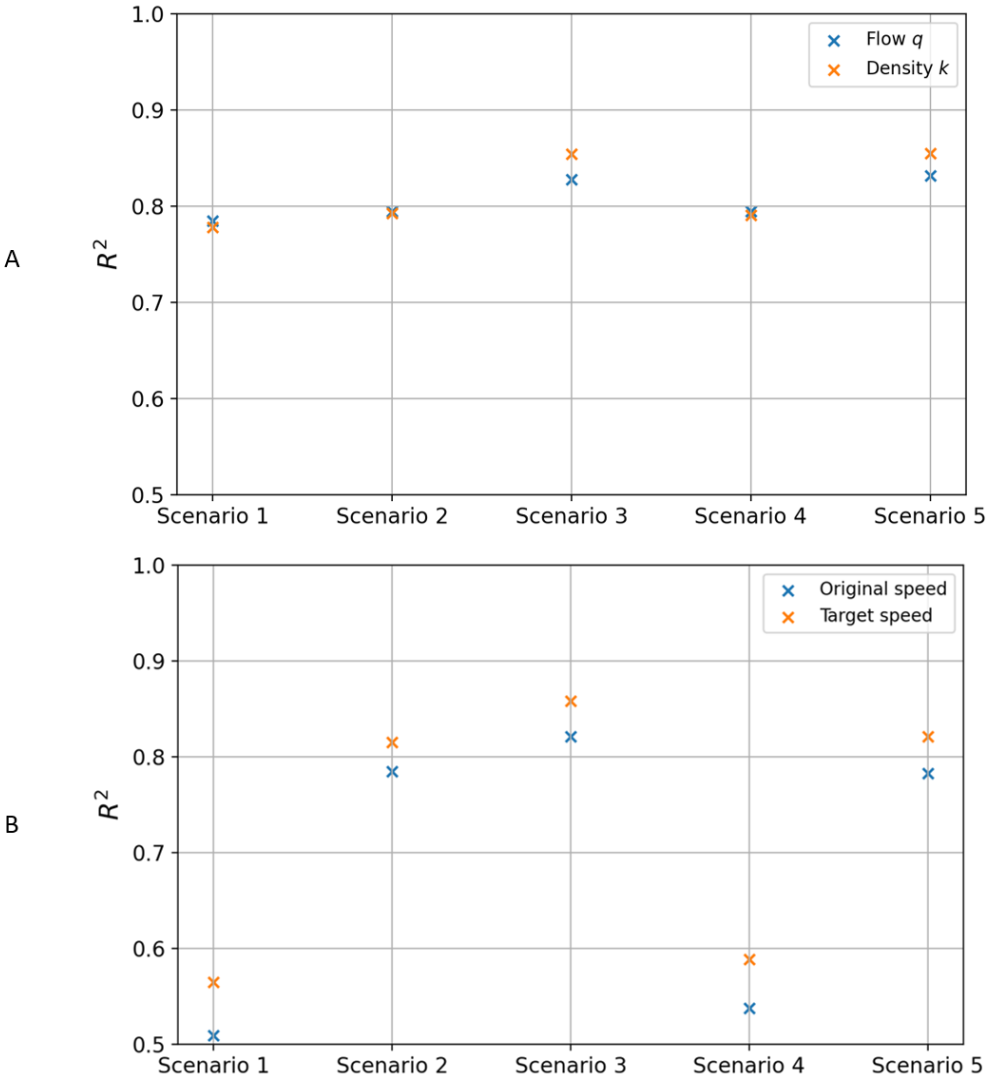

FIGURE 8: R^2 values for the estimated flow and density (A) and for the predicted speed compared to the target speed and the original speed (B) per scenario.

to an R2 score of 0.72. In contrast to the results for the canonical parameters, the bus data also brings a significant improvement to a value of about 0.65, but is still not as good as using taxi data. Since the considered stops are performed just exactly by buses, besides taxis and delivery vehicles, but the flow, density and speed capture all modes, this improvement for the extended variables fits the expected result. The better prediction with taxi data can be explained by the significantly higher share of taxis compared to buses. Noticable here is that the number of lane changes seems to be more affected by buses than by taxis. Despite the different proportions, the estimate here is slightly better for the bus data. When all data sources are available, the result for the stops is the best. Consequently, scenario 5, which combines all data, i.e. LD, FCD, taxi and bus data, delivers the best result with an R2 value of almost 0.8.

In summation, considering the flow, density and speed estimation as well as the extended information, namely the number of stops and lane changes, scenario 5 offers the best results.

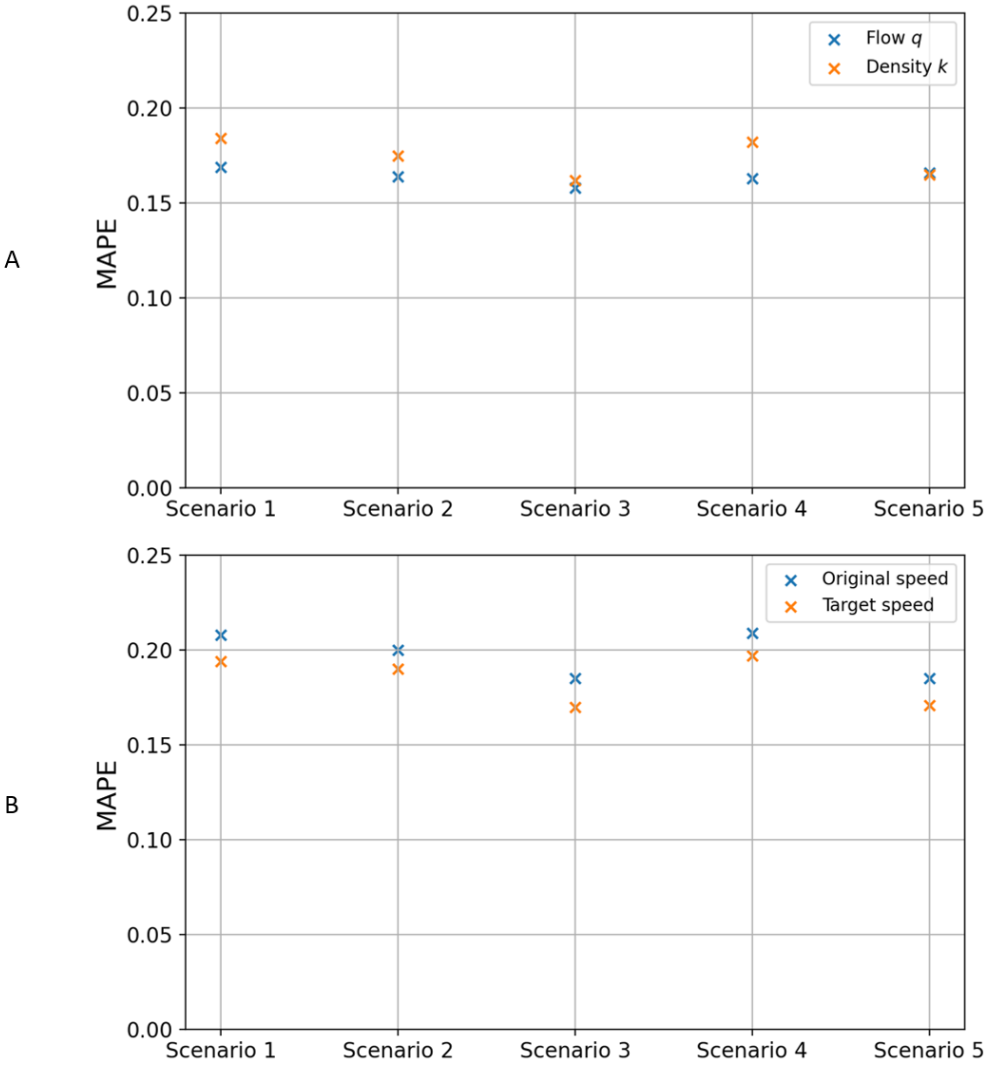

FIGURE 9: MAPE calculated for the estimated flow und density (D) and the speed compared to the target and the original speed (E) per scenario.

Having, besides the LD and FCD only the bus data available leads to a significant deterioration for the speed estimation. Therefore, scenario 3, using only taxi data as further source, is the more promising solution, but may be limited to cities that have this high share of taxis.

CONCLUSION

The results presented in this paper show that the extended traffic state provides further information on the complexity of urban traffic. Using advances in data collection and physics-informed deep learning, we have further shown how to extend the traffic state, which is typically described in terms of flow, density and speed, to include the stops of delivery vehicles, buses and taxis, as well as the number of lane changes, as well as how to estimate it. Using the proposed method applied to different currently existing sensor distributions of loop detector and trajectory data sources (FCD, taxis, buses), we have shown how the extended traffic state estimation performs under different scenarios of sensor data availability. Our findings help to perform and reproduce the extended traf-

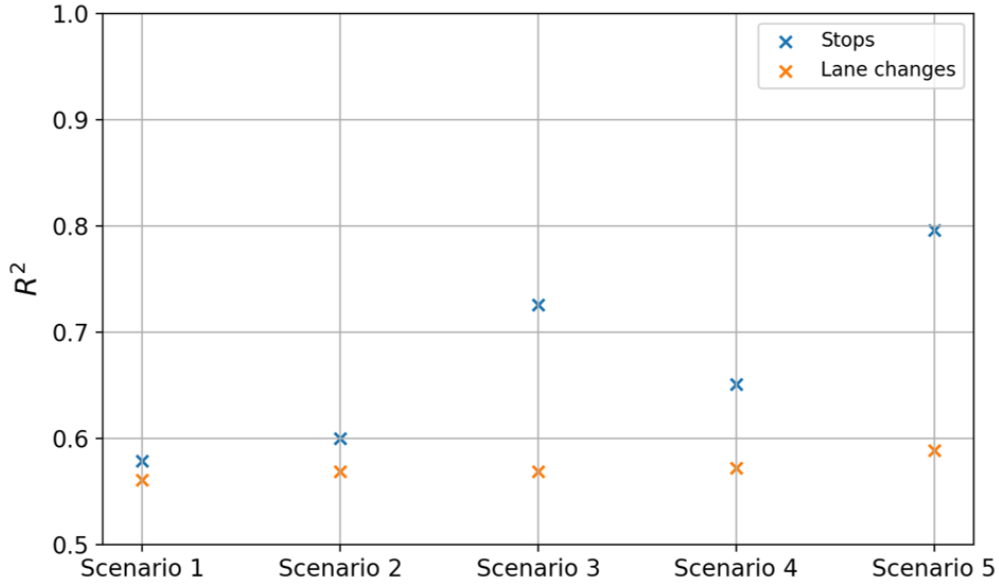

FIGURE 10: R^2 values for the estimated number and the number of lane changes per scenario.

fic state estimation elsewhere around the world. The proposed approach has practical applications. Examples are found, for example, in routing, where segments with an increased number of stops can be assigned higher costs in the shortest path algorithm. In addition, the insights can be used in planning, since a network-wide estimation of lane changes on links can be used for a safety assessment. These applications will be explored in future research.

Future research will also concentrate on extending the presented idea to out-of-sample predictions. In other words, training the estimation method on a subset of links and predicting it on the entire network. Since the static features are known and the dynamic features can be observed by existing measurement technologies, we expect that these out-of-sample predictions are possible at acceptable errors. It will be also addressed whether calibrated networks can be extended to other road categories or even other cities and countries. However, the currently available data are still too limited. A sample as comprehensive as pNEUMA from Athens, which covers such a large interconnected network, does not exist.

In closing, the presented extended traffic state is a promising approach to describe and understand the complexity of urban traffic phenomena at the link level that help decision makers to take more informed decisions.

ACKNOWLEDGMENTS

Data source: pNEUMA – open-traffic.epfl.ch. Alexander Kutsch acknowlegdes support from the German Federal Ministry for Digital and Transport (BMDV) for the funding of the project TEMPUS (Test Field Munich - Pilot Test Urban Automated Road Traffic), grant no. 01MM20008K. Allister Loder acknowledges support from the German Federal Ministry for Digital and Transport (BMDV) for the funding of the project KIVI (Artificial Intelligence in Ingolstadt's Transportation System), grant no. 45KI05A011. Furthermore, we wish to acknowledge the assistance provided by Victoria Dahmen.

AUTHOR CONTRIBUTIONS

The authors confirm contribution to the paper as follows. **Alexander Kutsch:** Conceptualization, Methodology, Software, Formal Analysis, Data Curation, Writing - Original Draft, Visualization **Allister Loder:** Conceptualization, Methodology, Data Curation, Writing - Original Draft **Gabriel Tilg:** Conceptualization, Methodology, Writing - Review & Editing **Klaus Bogenberger:** Writing - Review & Editing, Supervision, Funding acquisition. All authors reviewed the results and approved the final version of the manuscript.

References

1. Zhao, J., Z. Yi, S. Pan, Y. Zhao, Z. Zhao, F. Su, and B. Zhuang, Unsupervised Traffic Anomaly Detection Using Trajectories. In *CVPR Workshops*, 2019, pp. 133–140.
2. Santhosh, K. K., D. P. Dogra, P. P. Roy, and A. Mitra, Vehicular Trajectory Classification and Traffic Anomaly Detection in Videos Using a Hybrid CNN-VAE Architecture. *IEEE Transactions on Intelligent Transportation Systems*, 2021, pp. 1–12.
3. Seo, T., A. M. Bayen, T. Kusakabe, and Y. Asakura, Traffic state estimation on highway: A comprehensive survey. *Annual Reviews in Control*, Vol. 43, 2017, pp. 128–151.
4. Deng, W., H. Lei, and X. Zhou, Traffic state estimation and uncertainty quantification based on heterogeneous data sources: A three detector approach. *Transportation Research Part B: Methodological*, Vol. 57, 2013, pp. 132–157.
5. Kong, Q.-J., Z. Li, Y. Chen, and Y. Liu, An Approach to Urban Traffic State Estimation by Fusing Multisource Information. *IEEE Transactions on Intelligent Transportation Systems*, Vol. 10, No. 3, 2009, pp. 499–511.
6. Wang, Y., M. Papageorgiou, and A. Messmer, Real-Time Freeway Traffic State Estimation Based on Extended Kalman Filter: A Case Study. *Transportation Science*, Vol. 41, No. 2, 2007, pp. 167–181.
7. Van Lint, J., S. P. Hoogendoorn, and A. Hegyi, Dual EKF State and Parameter Estimation in Multi-Class First-Order Traffic Flow Models. *IFAC Proceedings Volumes*, Vol. 41, No. 2, 2008, pp. 14078–14083, 17th IFAC World Congress.
8. Treiber, M. and D. Helbing, An adaptive smoothing method for traffic state identification from incomplete information. In *Interface and Transport Dynamics*, Springer, Berlin, Heidelberg, 2003, pp. 343–360.
9. Herrera, J. C. and A. M. Bayen, Incorporation of Lagrangian measurements in freeway traffic state estimation. *Transportation Research Part B: Methodological*, Vol. 44, No. 4, 2010, pp. 460–481.
10. Yuan, Y., *Lagrangian Multi-Class Traffic State Estimation*. dissertation, Delft University of Technology, 2013.
11. Antoniou, C., H. N. Koutsopoulos, and G. Yannis, Dynamic data-driven local traffic state estimation and prediction. *Transportation Research Part C: Emerging Technologies*, Vol. 34, 2013, pp. 89–107.
12. Belzner, H., K. Bogenberger, and R. Kates, A Hybrid Model for Forecasting Local Traffic Parameters. *IFAC Proceedings Volumes*, Vol. 36, No. 14, 2003, pp. 269–273, 10th IFAC Symposium on Control in Transportation Systems 2003, Tokyo, Japan, 4-6 August 2003.
13. Hiribarren, G. and J. C. Herrera, Real time traffic states estimation on arterials based on trajectory data. *Transportation Research Part B: Methodological*, Vol. 69, 2014, pp. 19–30.

14. Pun, L., P. Zhao, and X. Liu, A Multiple Regression Approach for Traffic Flow Estimation. *IEEE Access*, Vol. 7, 2019, pp. 35998–36009.
15. Tišljarić, L., T. Carić, B. Abramović, and T. Fratrović, Traffic State Estimation and Classification on Citywide Scale Using Speed Transition Matrices. *Sustainability*, Vol. 12, No. 18, 2020.
16. Rostami Shahrbabaki, M., A. A. Safavi, M. Papageorgiou, and I. Papamichail, A data fusion approach for real-time traffic state estimation in urban signalized links. *Transportation Research Part C: Emerging Technologies*, Vol. 92, 2018, pp. 525–548.
17. Kumar, N. and M. Raubal, Applications of deep learning in congestion detection, prediction and alleviation: A survey. *Transportation Research Part C: Emerging Technologies*, Vol. 133, 2021, p. 103432.
18. Raissi, M., P. Perdikaris, and G. E. Karniadakis, Physics Informed Deep Learning (Part I): Data-driven Solutions of Nonlinear Partial Differential Equations. *arXiv preprint arXiv:1711.10561*, 2017.
19. Raissi, M., P. Perdikaris, and G. E. Karniadakis, Physics Informed Deep Learning (Part II): Data-driven Discovery of Nonlinear Partial Differential Equations. *arXiv preprint arXiv:1711.10566*, 2017.
20. Raissi, M., P. Perdikaris, and G. E. Karniadakis, Physics-informed neural networks: A deep learning framework for solving forward and inverse problems involving nonlinear partial differential equations. *Journal of Computational Physics*, Vol. 378, 2019, pp. 686–707.
21. Um, K., R. Brand, Yun, Fei, P. Holl, and N. Thuerey, Solver-in-the-Loop: Learning from Differentiable Physics to Interact with Iterative PDE-Solvers, 2020.
22. Akwir, N. A., J. C. Chedjou, and K. Kyamakya, Neural-Network-Based Calibration of Macroscopic Traffic Flow Models BT - Recent Advances in Nonlinear Dynamics and Synchronization: With Selected Applications in Electrical Engineering, Neurocomputing, and Transportation. Springer International Publishing, Cham, 2018, pp. 151–173.
23. Huang, J. and S. Agarwal, Physics Informed Deep Learning for Traffic State Estimation. *2020 IEEE 23rd International Conference on Intelligent Transportation Systems, ITSC 2020*, 2020.
24. Yuan, Y., X. T. Yang, Z. Zhang, and S. Zhe, *Macroscopic traffic flow modeling with physics regularized Gaussian process: A new insight into machine learning applications*, 2021.
25. Liu, J., M. Barreau, M. Čičić, and K. H. Johansson, Learning-based traffic state reconstruction using Probe Vehicles. *arXiv*, 2020.
26. Shi, R., Z. Mo, K. Huang, X. Di, and Q. Du, Physics-Informed Deep Learning for Traffic State Estimation, 2021.
27. Shi, R., Z. Mo, and X. Di, Physics-Informed Deep Learning for Traffic State Estimation : A Hybrid Paradigm Informed By Second-Order Traffic Models, 2021.
28. Rempe, F., A. Loder, and K. Bogenberger, Estimating motorway traffic states with data fusion and physics-informed deep learning. *IEEE Intelligent Transportation Systems Conference (ITSC)*, 2021.
29. Dahmen, V., A. Loder, G. Tilg, A. Kutsch, and K. Bogenberger, Traffic State Estimation with Loss Constraint. *IEEE Intelligent Transportation Systems Conference (ITSC)*, 2022, accepted.

30. Barmpounakis, E. and N. Geroliminis, On the new era of urban traffic monitoring with massive drone data: The pNEUMA large-scale field experiment. *Transportation Research Part C: Emerging Technologies*, Vol. 111, No. November 2019, 2020, pp. 50–71.
31. Pandey, A., M. Sharma, and S. Biswas, Concept of heterogeneity index for urban mixed traffic. *International Journal of Transportation Science and Technology*, 2022.
32. Loder, A., L. Bressan, M. J. Wierbos, H. Becker, A. Emmonds, M. Obee, V. L. Knoop, M. Menendez, and K. W. Axhausen, How Many Cars in the City Are Too Many? Towards Finding the Optimal Modal Split for a Multi-Modal Urban Road Network. *Frontiers in Future Transportation*, Vol. 2, No. May, 2021.
33. Loder, A., T. Otte, and K. Bogenberger, Using Large-Scale Drone Data to Monitor and Assess the Behavior of Freight Vehicles on Urban Level. *Transportation Research Record*, Vol. 0, No. 0, 0, p. 03611981221093620.
34. Xue, Q., Y. Xing, and J. Lu, An integrated lane change prediction model incorporating traffic context based on trajectory data. *Transportation Research Part C: Emerging Technologies*, Vol. 141, 2022, p. 103738.
35. Kesting, A., M. Treiber, and D. Helbing, General Lane-Changing Model MOBIL for Car-Following Models. *Transportation Research Record*, Vol. 1999, No. 1, 2007, pp. 86–94.
36. Zhao, H.-T., H.-Z. Li, H. Qin, and L.-H. Zheng, Two-lane mixed traffic flow model considering lane changing. *Journal of Computational Science*, Vol. 61, 2022, p. 101635.
37. Raj, P., G. Asaithambi, and A. Ravi Shankar, Effect of curbside bus stops on passenger car units and capacity in disordered traffic using simulation model. *Transportation Letters*, 2022.
38. Wang, R., S. Fan, and D. B. Work, Efficient multiple model particle filtering for joint traffic state estimation and incident detection. *Transportation Research Part C: Emerging Technologies*, Vol. 71, 2016, pp. 521–537.
39. Weil, R., J. Wootton, and A. García-Ortiz, Traffic incident detection: Sensors and algorithms. *Mathematical and Computer Modelling*, Vol. 27, No. 9, 1998, pp. 257–291.
40. Gazis, D. C. and R. Herman, The Moving and "Phantom" Bottlenecks. *Transportation Science*, Vol. 26, No. 3, 1992, pp. 223–229.
41. Coifman, B., S. Krishnamurthy, and X. Wang, Lane-Change Maneuvers Consuming Freeway Capacity. In *Traffic and Granular Flow '03* (S. P. Hoogendoorn, S. Luding, P. H. L. Bovy, M. Schreckenberg, and D. E. Wolf, eds.), Springer Berlin Heidelberg, Berlin, Heidelberg, 2005, pp. 3–14.
42. Barmpounakis, E., G. M. Sauvin, and N. Geroliminis, Lane Detection and Lane-Changing Identification with High-Resolution Data from a Swarm of Drones. *Transportation Research Record*, Vol. 2674, No. 7, 2020, pp. 1–15.
43. Edie, L., Discussion of Traffic Stream Measurements and Definitions. In *Proceedings of the 2nd International Symposium on the Theory of Traffic Flow*, 1963, p. 139–154.
44. Bishop, C. M., Neural networks and their applications. *Review of Scientific Instruments*, Vol. 65, No. 6, 1994, pp. 1803–1832.